Resistive model of the rf discharge including additional dc currents and electrodes

Michael Klick
Adolf-Slaby-Institut, Slabystrasse 7a, D-O-1160 Berlin, Federal Republic of Germany
(Received 30 July 1992)

A resistive model including additional dc currents and electrodes enables understanding and analysis of rf discharges in the low-frequency range ($\omega \ll \omega_{pi}$). A general and exact analysis based on asymptotic solutions results in analytic representations of relations between sheath voltages, bias, and rf voltage. For sinusoidal rf voltage an expansion of sheath voltages and discharge current into Fourier series, e.g., important for probe measurements, and a general relation between these series is presented. From the power balance a lower bound of a sinusoidal rf voltage is derived. The model is extended for different densities and electron temperatures along the sheath edges. Correction and error estimation show the asymptotic solution to be well suited.

PACS number(s): 52.70.Gw, 52.75.−d, 52.65.+z, 52.80.Hc

I. INTRODUCTION

In the past ten years the rf discharge has come under increased scrutiny with the forced application of plasma-enhanced dry processing. For several applications the low-frequency regime considered in this paper ($\omega \ll \omega_{pi}$) is more convenient than the opposite regime using frequencies which exceed the ion plasma frequency ω_{pi} (e.g., $\omega/2\pi = 13.56$ MHz) essentially.

The resistive model presented in this paper implies boundary conditions often found in experiments. Probes [1], auxiliary electrodes [2,3], insulating layers, or other solid bodies with nonzero potential will be treated as additional electrodes. Special cases of various powered electrodes, e.g., 13.56 MHz on top or an auxiliary electrode to provide a high plasma density and 100 kHz on a lower electrode to adjust the ion energy, can also be characterized approximately.

Especially for the successful use of tuned [4,5] or high impedance [6,7] probe measurements with suppression of rf components in the probe characteristic, the knowledge of plasma potential, or its expansion in a Fourier series, may be desirable, or even necessary [8,9].

Most known investigations concerning this frequency range, such as were done by Godyak and Kuzovnikov [10], have focused their interest on the physical understanding of the properties of the discharge [11–13], or give only slightly different approximations of earlier models [14–16]. Only pure configurations with two electrodes and without an additional dc discharge current have been considered. An approach to a systematic and mathematically exact treatment based on asymptotic, i.e., analytical, solutions will be given in this work.

At low pressures, usual $p \lesssim 100$ Pa ~ 1 Torr, the Debye length λ_D is the smallest characteristic length of the plasma and the impedance of the discharge is dominated by the properties of the space-charge sheath (sheath) [10,17]. Due to the high electron temperature and very low mass ratio m_e/m_+ (mobility, thermal velocity) a sheath always exists at the plasma sheath boundary separating the quasineutral plasma from the confining surface consisting of walls, electrodes, or other solid bodies. The sheaths give rise to specific relations in current and voltage of the rf discharge. Depending on rf voltage and net current, the sheath has an extent of only a few up to several tens of λ_D [18].

The electric fields are of fundamental interest because the plasma potential, or in general the sheath voltage as the potential drop across the sheath, determines the ion energy distribution at the wall to a large extent [2,13,19]. At low pressures, when collisions can be neglected, and if the ion transit time is much shorter than the rf period, a complete dependence on the sheath voltage can be given.

In this case the discharge can be treated in a reduced form. The rf voltage decreased by the potential drop of the plasma (bulk) resistance can be introduced as an effective rf voltage. Hence the reduced discharge consists of sheaths only, and the plasma appears as a source of charge carriers with an infinite conductivity. Several important relations can be given without any assumption concerning a special effective rf voltage. At low pressures there is no essential difference between the rf voltage applied at the powered electrode and the effective rf voltage. After deriving general relations, a sinusoidal rf voltage will be assumed.

Instead of a pure geometric area ratio [13,14], the discharge will be characterized by an ion current ratio involving special effects in asymmetrical discharges (see Sec. II A).

II. MODEL

A. Physical assumptions

The basic assumption of every resistive model is the neglect of the displacement current. In simple diode configurations the presence of the displacement current in the sheath was treated by several workers approximately [15,20]. Since these models are based on a quasistationary motion of ions, the ion density in the sheath is assumed to depend only on the potential with respect to the plasma. Neglecting ionization yields the total current

to be uniform within the sheath. Bearing this in mind and taking into account the quasineutrality of the plasma ($\omega \ll \omega_{pi} \ll \omega_{pe}$), the ionic displacement current at the electrode has to be small compared to the ionic convection current at the sheath boundary. Moreover, this model gives sheath expansion (or contraction) velocities which can exceed the ion velocity at the sheath boundary by orders of magnitude. The movement of the ion density profile in the sheath, and particularly at the boundary, however, has to be slower than the velocity of the ions at the sheath boundary given by the Bohm criterion [21–25]. Thus it can easily be shown that, according to the presheath mechanism, this ansatz gives only an insignificant or qualitative improvement in the frequency range of interest. This analysis suggests that, if the displacement cannot be neglected, it can be approximated by the pure electronic displacement current. Analytic estimations [26–28] and numerical [29] results confirm this assumption. An exact treatment requires a rigorous kinetic theory including the plasma body [25]. Simplified solutions of Boltzmann and Poisson equations show that the ionic convection current is modulated [29]. The obtained modulation is especially due to the fact that the ionic displacement current replenishes the sheath with ions when the sheath voltage decreases [30].

More important than a special ansatz for the displacement current is the condition that indicates whether the displacement current can be neglected or not. Because of strong nonlinearity in the relation between sheath voltage and conduction current, the usual condition $\omega \ll \omega_{pi}$ is very rough [27]. An exact condition can be given by a more general and analytical treatment [28].

For $\omega \ll \omega_{pi}$, however, a resistive model assuming a time-independent ion current should be a good approximation at least. The effect of the modulation of the ion current is discussed in the appendix.

In considering sheath and ambipolar diffusion we suppose a planar geometry and the plasma to consist only of electrons and positive ions [31]. Electrode separation and sheath width are assumed to be small compared to any other relevant geometric length. From this point of view the following assumptions will be made.

(a) The plasma density is constant in time. For a stationary plasma the frequency of ambipolar diffusion ν_D is equal to the ionization rate [32,33]. Thus a constant plasma density or current density, in particular in the neighborhood of the planar sheath boundary, requires a rf frequency ω exceeding ν_D by far. Experimental results confirm this approach [6,34].

In most cases charge exchange collisions are most important for the ion motion. At low ion velocities found in the bulk plasma of a gas discharge, the cross sections exceed those of other collisions, and they depend only slightly on velocity [33,35,36]. Hence, taking into account only such collisions, the free mean path λ_+ of the ions can be assumed as constant. Here the condition of constant plasma density can be expressed as [22,28,37–39]

$$\omega \gg \nu_D \approx \left[\frac{\lambda_+ k T_e}{m_+ L^3} \right]^{1/2} . \tag{1}$$

L is the half separation of the electrodes, T_e is the electron temperature, and m_+ denotes the ion mass.

(b) The electron temperature T_e, as a measure of mean electron energy, is constant in time. For rf frequencies well above the total energy dissipation frequency ν_e, harmonics of the isotropic electron distribution function can be neglected and T_e assumed to be independent of time. A sufficient reduction of harmonics can be expected for $\omega/p \rangle 10^3\ \mathrm{s^{-1}\ Pa^{-1}}$ (p is pressure in Pa) [6,40–43].

(c) Being mostly repelled, the thermal electrons are only slightly disturbed by wall losses and can be assumed to be in Boltzmann equilibrium. Electron density and current density in the sheath are therefore given by the Boltzmann relation. This assumption implies an electron distribution function similar or equal to the Boltzmann distribution and sheath voltages which do not fall below a critical value essentially [44–46]. Secondary electrons emitted at the electrode surface can be treated as a slight increase of the ion current which can be involved additionally (see Sec. III E).

According to the time-independent saturation current of ions I_{is} and electrons I_{es}, the current drawn by an electrode is

$$i = I_{is} + I_{es} \exp(-u/U_T) = I_{is}[1 - \exp(\eta_f - \eta)] , \tag{2}$$

where u is the sheath voltage, and $U_T = kT_e/e$ is the electron temperature in potential units. On the right-hand side of this equation the normalized sheath voltage $\eta = u/U_T$ and the normalized floating potential

$$\eta_f = \ln \frac{I_{es}}{I_{is}} = \ln \frac{j_{es}}{j_{is}} = \frac{1}{2} \ln \frac{m_+}{2\pi\kappa^2 m_e} \tag{3}$$

have been introduced. $\kappa = 1.247$ is the eigenvalue of the kinetic presheath theory for planar geometries assuming charge transfer collisions to be dominant [22,23]. The classical (hydrodynamical) Bohm criterion requires $\kappa = 1$ [24,47,48].

B. Basic equations

For the quantitative investigation dimensionless quantities with assumed positive directions are introduced in Fig. 1,

$$\eta_k = \frac{u_k}{U_T}, \quad \Gamma_k = \frac{i_k}{I_{is}^{(0)}} , \tag{4}$$

where $I_{is}^{(0)}$ is the ion current of the powered electrode. The ion current ratio α_k ($\alpha_0 = 1$) is defined as

$$\alpha_k = \frac{I_{is}^{(k)}}{I_{is}^{(0)}} = \frac{A_k \langle j_{is}^{(k)} \rangle_A}{A_0 \langle j_{is}^{(0)} \rangle_A} = \frac{A_k \langle n_0^{(k)} \rangle_A}{A_0 \langle n_0^{(0)} \rangle_A} \left[\frac{U_{Tk}}{U_{T0}} \right]^{1/2} , \tag{5}$$

the ratio of the area averaged current densities $\langle j_{is} \rangle_A$ at the sheath boundary and the geometrical area ratio. $n_0^{(k)}$ denotes the density at the sheath boundary of the kth electrode.

Accordingly the current at the kth electrode may now be written as

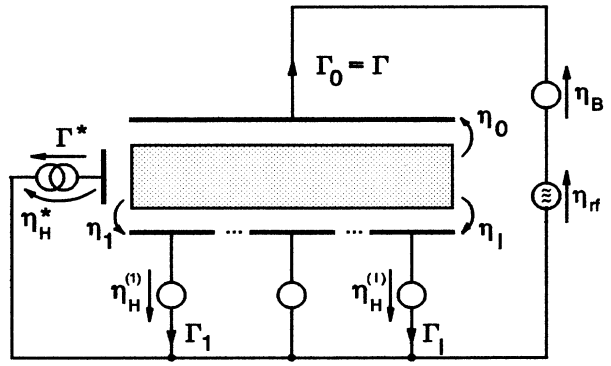

FIG. 1. Schematic outline of a rf discharge. The potential applied at l electrodes on the lower side is arbitrary, but fixed.

$$\frac{\Gamma_k}{\alpha_k} = 1 - \exp(\eta_f - \eta_k) \ . \tag{6}$$

The validity of the Boltzmann relation requires $\eta_k > 2$ [see assumption (c)].

The potential η_H in Fig. 1 is the time-independent electrode potential given by an external voltage, or a fixed mean electrode current, and remaining boundary conditions. Finally, the model is completed by an electrode carrying a constant current Γ^* and the time-dependent potential η^* (see Fig. 1).

An integral symmetry parameter is the sum of all α_k

$$\alpha = \sum_{k=1}^{l} \alpha_k + \Gamma^* \ . \tag{7}$$

Thus we can also take into consideration different ion current densities. This is just important for discharges which are not confined radially, and where the plasma volume varies with power, gas pressure, and gas type. Further on the power dissipated in the plasma and additional dc currents are scaled by the ion currents of the discharge. Thus the current density ratio α is a natural value for the characterization of rf discharges and should not be introduced as a pure geometrical area ratio which can be found in other investigations [10,12–15]. Due to the geometry of the chamber, the ion current ratio α appears to be dependent on pressure and rf power above all. Usually α decreases with higher pressures and lower power values [12,49].

Due to the quasineutrality of the plasma, a discharge system consisting of $l+1$ electrodes can be described, in conjunction with (6), by the following equations:

$$0 = \Gamma^* + \sum_{k=0}^{l} \Gamma_k \ , \tag{8}$$

$$\begin{aligned} &0 = \eta_q - \eta_0 + \eta_k + \eta_H^{(k)} \ , \\ &0 = \eta_H^{(r)} + \eta_r - \eta_H^{(p)} - \eta_p, \quad k,p,r = 1, \ldots, l \ . \end{aligned} \tag{9}$$

Inserting (6) and (8) yields

$$0 = \Gamma^* + \sum_{k=0}^{l} \alpha_k - \sum_{k=0}^{l} \alpha_k \exp(\eta_f - \eta_k) \ . \tag{10}$$

Combining with (9) and (7) provides the equation

$$0 = 1 + \alpha - \exp(\eta_f - \eta_0)[1 + a \exp(\eta_q)] \ , \tag{11}$$

where a is defined in terms of the electrode potentials $\eta_H^{(k)}$,

$$a = \sum_{k=1}^{l} \alpha_k \exp \eta_H^{(k)} \ , \tag{12}$$

and $\eta_q = \eta_B + \eta_{rf}$ is the potential of the driven electrode, α and a are integral symmetry parameters of a rf discharge, as shown in Fig. 1, determining both bias and sheath voltage.

C. Arbitrary rf voltages

For the discharge current $\Gamma = \Gamma_0$, one obtains from (6) and (11)

$$\Gamma = 1 - \frac{1+\alpha}{1 + a \exp(\eta_q)} \ . \tag{13}$$

Defining

$$B = \eta_B + \ln a \tag{14}$$

and rearranging (13), one obtains

$$\frac{1-\Gamma}{1+\alpha} = \frac{1}{1 + \exp(\eta_{rf} + B)} \ . \tag{15}$$

Inserting (9) into (10) yields

$$0 = 1 + \alpha - \exp(\eta_f - \eta_m - \eta_H^{(m)})[a + \exp(-\eta_q)] \ . \tag{16}$$

From Eqs. (6) and (13), one obtains a *linear* relation

$$1 - \frac{\Gamma_m}{\alpha_m} \exp(-\eta_H^{(m)}) = 1 - \frac{\Gamma_k}{\alpha_k} \exp(-\eta_H^{(k)}) = \frac{\alpha + \Gamma}{a} \tag{17}$$

between the currents drawn by arbitrary electrodes with fixed potential and, on the other hand, between these currents and the discharge current $\Gamma = \Gamma_0$. Time averaging and rearranging yields for $\ln a$,

$$\ln a = \ln \sum_{k=1}^{l} \alpha_k \exp(\eta_H^{(k)}) = \eta_H^{(m)} + \ln \frac{\alpha + \bar{\Gamma}}{1 - \bar{\Gamma}_m / \alpha_m} \ , \tag{18}$$

that this value is already determined by the average current $\bar{\Gamma} = \bar{\Gamma}_0$, potential, and the mean current of an arbitrary electrode m. Therefore the potential may be expressed as

$$\eta_H^{(m)}=\ln\sum_{\substack{k=1\\k\neq m}}^{l}\alpha_k\exp(\eta_H^{(k)})+\ln\frac{1-\bar{\Gamma}/\alpha_m}{\alpha-\alpha_m+\bar{\Gamma}+\bar{\Gamma}_m}\ . \tag{19}$$

It is very interesting to consider the usual case when bias current, ion current ratio, and rf voltage are independent of bias voltage:

$$\frac{d\bar{\Gamma}}{d\eta_B}=0,\quad \frac{d\alpha}{d\eta_B}=0,\quad \frac{\partial\eta_{\rm rf}}{\partial\eta_B}\equiv 0\ . \tag{20}$$

Capacitive coupling is included by $\bar{\Gamma}=0$. Integrating in time $\varphi=\omega t$ and taking the derivate with respect to η_B of (15) provides

$$0=\frac{d}{d\eta_B}\frac{1-\bar{\Gamma}}{1+\alpha}=\frac{1}{2\pi}\left[1+\frac{d\ln a}{d\eta_B}\right]\int_{2\pi}\frac{-\exp[\eta_q(\varphi)+\ln a\,]d\varphi}{\{1+\exp[+\eta_q(\varphi)+\ln a\,]\}^2}\ , \tag{21}$$

if we assume a functional dependence of η_B and $\ln a$ [see Eq. (12)]. Due to the non zero integral, one obtains, finally,

$$\frac{d\ln a}{d\eta_B}=-1\ . \tag{22}$$

This is an important relation between the electrode potentials $\eta_H^{(m)}$ $(m\geq 1)$ included in a and the bias voltage η_B.

Using Eq. (11), the sheath voltage of the driven electrode η_0 may be written as

$$\begin{aligned}\eta_0&=\eta_f-\ln(1+\alpha)+\ln\{1+\exp(\eta_q+\ln a)\}\\&=\eta_f-\ln(1+\alpha)+\eta_{\rm rf}+B+\ln\{1+\exp(-\eta_{\rm rf}-B)\}\end{aligned} \tag{23}$$

and for η_m $(m\neq 0)$

$$\begin{aligned}\eta_m&=\eta_f-\eta_H^{(m)}+\ln\frac{a}{1+\alpha}+\ln\{1+\exp(-\eta_q-\ln a)\}\\&=\eta_f-\eta_H^{(m)}+\ln\frac{a}{1+\alpha}+\ln\{1+\exp(-\eta_{\rm rf}-B)\}\ .\end{aligned} \tag{24}$$

Before a detailed calculation of the sheath voltages, general results can be derived by using (22) and appropriate boundary conditions (20). The derivate of η_0 according to (23)

$$\frac{\partial\eta_0}{\partial\eta_B}\equiv 0,\quad \frac{d\bar{\eta}_0}{d\eta_B}=0 \tag{25}$$

exhibits that the sheath voltage η_0 as a function in time φ (and so also on average) does not depend on alteration of the bias voltage caused by alteration of electrode potentials $\eta_H^{(m)}$ $(m\neq 0)$.

Using (9) and (25) or (24), for all $m\neq 0$ one obtains

$$\frac{\partial(\eta_m+\eta_H^{(m)})}{\partial\eta_B}\equiv -1,\quad \frac{d(\bar{\eta}_m+\eta_H^{(m)})}{d\eta_B}=-1\ . \tag{26}$$

To give a clear idea of the results of this very formal analysis, the case of vanishing average discharge current, so that $\bar{\Gamma}=0$, should be discussed. This case can be realized by the usual capacitive coupling of the powered electrode. A slowly variable potential is applied to an arbitrary electrode. If this potential is increased, the bias voltage decreases. Looking at another electrode m with a fixed potential $\eta_H^{(m)}$, the sheath voltage grows as much as the bias voltage declines. Consequently, the bias voltage is a *linear* measure for the increase of the sheath voltage caused by a different electrode with growing potential. According to (25), the sheath voltage η_0 will not be influenced.

III. SINUSOIDAL rf VOLTAGES

A. Mathematical solution

If we suppose, in agreement with experimental experience [6,41,43], the rf voltage to be a sinusoidal function of reduced time $\varphi=\omega t$,

$$\eta_q(\varphi)=\eta_{\rm rf}+\eta_B=\hat{\eta}\cos\varphi+\eta_B\ , \tag{27}$$

the right-hand side of (13) can be represented by the Fourier expansion

$$\Gamma=1-\frac{1+\alpha}{2}\sum_{n=-\infty}^{\infty}G_n\exp(in\varphi)\ , \tag{28}$$

where the coefficients G_n of the complex Fourier series of the discharge current are defined by

$$G_n=\frac{2}{\pi}\int_0^{\pi}\frac{\cos n\varphi\,d\varphi}{1+\exp(\hat{\eta}\cos\varphi+B)}\ . \tag{29}$$

At bias voltages, which does not exceed the rf peak voltage, strictly speaking $|B|\leq\hat{\eta}$, it is convenient to introduce the angle of (positive) current flow according to Fig. 2,

$$\tilde{\varphi}=\arccos(-B/\hat{\eta})\ , \tag{30}$$

and to split integrand and integration interval

$$\begin{aligned}G_n=&\frac{2}{\pi}\int_0^{\tilde{\varphi}}\frac{\cos n\varphi\,d\varphi}{1+\exp(\hat{\eta}\cos\varphi+B)}\\&+\frac{2}{\pi}\int_{\tilde{\varphi}}^{\pi}\left[1-\frac{\exp(\hat{\eta}\cos\varphi+B)}{1+\exp(\hat{\eta}\cos\varphi+B)}\right]\cos n\varphi\,d\varphi\ .\end{aligned} \tag{31}$$

Carrying out the first part of the second integral yields

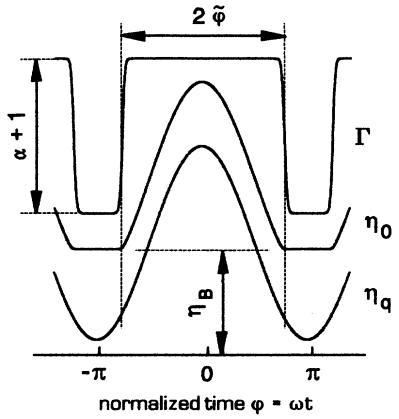

FIG. 2. Discharge current Γ, sinusoidal discharge voltage η_q, and sheath voltage η_0 for $B>0$ (qualitative).

$$G_n=\frac{2}{\pi}\left[\frac{\sin n\varphi}{n}\Bigg|_{\tilde{\varphi}}^{\pi}+\int_0^{\tilde{\varphi}}\frac{\cos n\varphi\,d\varphi}{1+\exp(\hat{\eta}\cos\varphi+B)}-\int_{\tilde{\varphi}}^{\pi}\frac{\cos n\varphi\,d\varphi}{1+\exp(-\hat{\eta}\cos\varphi-B)}\right]. \tag{32}$$

If $\hat{\eta}\to\infty$ and $B/\hat{\eta}<1$, so that $\tilde{\varphi}\in[0,\pi]$, the integrands are vanishing excluding one single point at $\varphi=\tilde{\varphi}$. Hence we obtain the asymptotic representation of G_n immediately:

$$\frac{1}{2}G_0=1-\frac{\tilde{\varphi}}{\pi}=\frac{1}{\pi}\arccos\frac{B}{\hat{\eta}}\,, \tag{33}$$

$$G_n=-\frac{2}{\pi n}\sin n\tilde{\varphi},\quad \forall n\neq 0\,. \tag{34}$$

For $|B|\rangle\hat{\eta}$ the asymptotic representation can be taken from (29) directly,

$$\frac{G_0}{2}=\begin{cases}0, & \forall B>\hat{\eta}\\ 1, & \forall B<-\hat{\eta}\,.\end{cases} \tag{35}$$

For $|B|\rangle\hat{\eta}$ and $n\neq 0$, Eq. (29) provides $G_n=0$.

Supposing $|B|\langle\hat{\eta}$ and finite $\hat{\eta}$, the error estimation ΔG_0 for the asymptotic representation of G_0 is given by

$$\frac{\Delta G_0}{2}=\frac{1}{\pi}\int_0^{\tilde{\varphi}}\frac{d\psi}{1+\exp(\hat{\eta}\cos[\tilde{\varphi}-\psi]+B)}-\frac{1}{\pi}\int_0^{\pi-\tilde{\varphi}}\frac{d\psi}{1+\exp(-\hat{\eta}\cos[\tilde{\varphi}+\psi]-B)}\,. \tag{36}$$

For the sake of further simplicity the conditions $|\tilde{\varphi}-\pi/2|\neq\pi/2$ and $\hat{\eta}\gg 1$ are supposed.

$$\frac{\Delta G_0}{2}\approx\frac{1}{\pi}\int_0^{\pi/2-|\tilde{\varphi}-\pi/2|}\frac{-\sinh\{B(1-\cos\psi)\}\,d\psi}{\cosh\{B(1-\cos\psi)\}+\cosh\{\hat{\eta}\sin\tilde{\varphi}\sin\psi\}}\,. \tag{37}$$

Finally, a Taylor expansion for small φ and $|B/\hat{\eta}|\neq 1$ provides the error correction ΔG_0,

$$\frac{\Delta G_0}{2}\approx-\frac{2B}{\pi(\hat{\eta}\sin\tilde{\varphi})^3}=-\frac{2B}{\pi(\hat{\eta}^2-B^2)^{3/2}}\,, \tag{38}$$

for finite $\hat{\eta}$ and B. This relation shows the essential properties of the asymptotic representation of G_0. At $B=0$ there is no error. Only close to the matching point of (33) and (35), at $|B|\approx\hat{\eta}(|\tilde{\varphi}-\pi/2|\approx\pi/2)$, the error correction ΔG_0 indicates an error worth mentioning. At large $|B|>\hat{\eta}$ the asymptotic representation approaches the exact solution rapidly. An improvement of the asymptotic solution appears to be required in the neighborhood of the matching point only. In agreement to the asymptotic representation of G_n,

$$\frac{1}{\pi}\int_{2\pi}\frac{\exp(-in\varphi)d\varphi}{1+\exp(\hat{\eta}\cos\varphi+B)}=2\delta_{0n}-\frac{(-1)^n}{\pi}\int_{\pi}\frac{\exp(-in\varphi)d\varphi}{1+\exp(\hat{\eta}\cos\varphi-B)}\,, \tag{39}$$

it is sufficient to derive the solution for $B\geq\hat{\eta}>0$ alone. δ_{kl} designates the Kronecker symbol which is usually defined to be

$$\delta_{kl}=\begin{cases}1, & \forall k=l\\ 0, & \forall k\neq l\,.\end{cases} \tag{40}$$

In order to obtain an asymptotic representation, Eq. (29) can be expanded into a Taylor series

$$G_n=\frac{1}{\pi}\int_{2\pi}\frac{\exp(-\hat{\eta}\cos\varphi-B-in\varphi)}{1+\exp(-\hat{\eta}\cos\varphi-B)}d\varphi=\frac{1}{\pi}\int_{2\pi}\sum_{k=1}^{\infty}(-1)^{k-1}\exp[-k(\hat{\eta}\cos\varphi+B)-in\varphi]d\varphi\,, \tag{41}$$

where the integral can be replaced by the integral representation of the modified Bessel function of the first kind I_n. The asymptotic expansion of I_n is

$$I_n(z)=\frac{[\mathrm{sgn}(z)]^n\exp|z|}{\sqrt{2\pi|z|}}\left[1+O\left[\frac{1}{|z|}\right]\right]. \tag{42}$$

The sign of z is given by sgn, and n designates the order of the Bessel function. Using the known integral representation of I_n and (42), the integral in (41) can be replaced by $\hat{\eta}\gg 1$.

$$G_n = 2(-1)^n \sum_{k=1}^{\infty} (-1)^{k-1} \exp(-kB) I_n(k\hat{\eta})$$

$$= 2(-1)^n \sum_{k=1}^{\infty} \exp[k(\hat{\eta}-B)] \frac{(-1)^{k-1}}{\sqrt{2\pi k\hat{\eta}}} . \quad (43)$$

This alternating series is convergent if

$$D = \exp(\hat{\eta}-B) \leq 1 . \quad (44)$$

At $D=1$ one obtains numerically (rounded)

$$K_1 = \sum_{k=1}^{\infty} \frac{(-1)^{k-1}}{\sqrt{k}} = 0.6049 . \quad (45)$$

The series in (43) converges very slowly. An approximation using the first two terms is only useful for $D < 0.1$. The limiting value of (43) can be approximated by that of the similar geometric series which is obtained by removing the square-root term. This interpolation

$$\sum_{k=1}^{\infty} \frac{(-1)^{k-1}}{\sqrt{k}} D^k \approx \frac{1}{K_1^* + 1/D} , \quad (46)$$

where $K_1^* = 1/K_1 - 1 = 0.6532$, gives the exact value for $\hat{\eta} = B(D=1)$ and $B/\hat{\eta} \to \infty (D \to 0)$. An additional correction for finite values of $\hat{\eta}$ was obtained numerically and replaces $\hat{\eta}$ by $\hat{\eta} - \frac{1}{3}$. The solution for $B \geq \hat{\eta} > 0$ can be expressed as

$$G_n = \frac{2(-1)^n}{\sqrt{2\pi(\hat{\eta}-1/3)}[K_1^* + \exp(B-\hat{\eta})]} . \quad (47)$$

Hence, in conjunction with (39), for $-B \geq \hat{\eta} > 0$

$$G_n = 2\delta_{0n} - \frac{2(-1)^n}{\sqrt{2\pi(\hat{\eta}-1/3)}[K_1^* + \exp(-B-\hat{\eta})]} . \quad (48)$$

These relations show that the error of the asymptotic solution for $|B| < \hat{\eta}$ is, instead of $O(\hat{\eta}^{-2})$ given by (38) for $|B| < \hat{\eta}$, of $O(\hat{\eta}^{-1/2})$. Finally, the matching point B^* with the asymptotic representation (33) and (34) have to be determined. The asymptotic representation supplies $G_n = 0$ for $B = \hat{\eta}$ incompatible with (47) for finite $\hat{\eta}$. Fortunately, formula (47) is also a good approximation outside the convergence domain ($B \geq \hat{\eta}$) given by condition (46). A conventional matching is obtained for $B^* = \hat{\eta} - 1$ which was confirmed by a numerical calculation. For $B < 0$ the analogous point is $B = -B^*$.

In considering the sheath voltage, the term depending on $\eta_q(\varphi)$ in (23) and (24) can be represented by the Fourier series

$$\ln\{1+\exp(-\hat{\eta}\cos\varphi - B)\} = \frac{1}{2} \sum_{n=-\infty}^{\infty} H_n \exp(in\varphi) \quad (49)$$

and

$$H_n = \frac{1}{\pi} \int_{2\pi} \ln\{1+\exp(-\hat{\eta}\cos\varphi - B)\} \exp(-in\varphi) d\varphi . \quad (50)$$

By differentiation with respect to B

$$\frac{dH_n}{dB} = -\frac{1}{\pi} \int_{2\pi} \frac{\exp(-in\varphi) d\varphi}{1+\exp(\hat{\eta}\cos\varphi + B)} , \quad (51)$$

the calculation of the coefficients H_n can be reduced to the derivation of G_n (C_n is the integration constant)

$$H_n = -\int G_n dB + C_n . \quad (52)$$

It can be shown that the validity of this relation is not restricted to a sinusoidal rf voltage. Inserting (34) yields the asymptotic representation ($\hat{\eta} \to \infty$)

$$H_n = \frac{2}{n\pi} \int \sin n\tilde{\varphi}\, dB + C_n$$

$$= \frac{2\hat{\eta}}{n\pi} \int \sin n\tilde{\varphi} \sin\tilde{\varphi}\, d\tilde{\varphi} + C_n , \quad (53)$$

where $|n| \neq 0$ and $\tilde{\varphi} \in [0, \pi]$. The asymptotic representations of (50) and (52) are steady with respect to B, including $|B| = \hat{\eta}$. Therefore the integration constant C_n vanishes for all $|n| \neq 1$. Bearing this in mind, one obtains for $|n| \geq 2$

$$H_n = \frac{\hat{\eta}}{n\pi} \left[\frac{\sin(n-1)\tilde{\varphi}}{n-1} - \frac{\sin(n+1)\tilde{\varphi}}{n+1} \right] , \quad (54)$$

for $|n| = 1$

$$H_1 = \hat{\eta} \left[\frac{\tilde{\varphi}}{\pi} - 1 - \frac{\sin 2\tilde{\varphi}}{2\pi} \right] , \quad (55)$$

and for $n = 0$ from (33) and (52)

$$\frac{H_0}{2} = \hat{\eta} \left[\left[1 - \frac{\tilde{\varphi}}{\pi} \right] \cos\tilde{\varphi} + \frac{\sin\tilde{\varphi}}{\pi} \right]$$

$$= \frac{1}{\pi} \left[(\hat{\eta}^2 - B^2)^{1/2} - B \arccos\frac{B}{\hat{\eta}} \right] . \quad (56)$$

In the case of $|B| > \hat{\eta}$, the asymptotic representation follows from (35) or (50). At $n = 0$ the coefficient H_n becomes

$$\frac{H_0}{2} = \begin{cases} 0, & \forall B > \hat{\eta} \\ -B, & \forall -B > \hat{\eta} \end{cases} \quad (57)$$

and vanishes for $n \neq 0$. Substituting from (38) into (52), we find the error correction ΔH_0 of the asymptotic solution for finite $\hat{\eta}$

$$\frac{\Delta H_0}{2} \approx \frac{2}{\pi} \int \frac{B\, dB}{(\hat{\eta}^2 - B^2)^{3/2}} = \frac{2}{\pi(\hat{\eta}^2 - B^2)^{1/2}} . \quad (58)$$

Note that ΔH_0 is of $O(\hat{\eta}^{-1})$. Analogous to ΔG_0 given by (38) this relation indicates essential properties of the asymptotic solution. At $B = 0$ the error becomes minimal and grows essentially only if $|B| \approx \hat{\eta}$ ($|\tilde{\varphi} - \pi/2| \approx \pi/2$). For $|B| > \hat{\eta}$ the asymptotic solution approaches the exact one. For the correction of the asymptotic solution at $|B| \approx \hat{\eta}$ an equation analogous to (39) can be derived:

$$\frac{1}{\pi}\int_{2\pi}\ln\{1+\exp(-\hat{\eta}\cos\varphi-B)\}\exp(-in\varphi)d\varphi=\frac{(-1)^n}{\pi}\int_{2\pi}\ln\{1+\exp(-\hat{\eta}\cos\varphi+B)\}\exp(-in\varphi)d\varphi-2\delta_{0n}B-\delta_{1n}\hat{\eta}\ . \tag{59}$$

Therefore the following derivation can be restricted to the range $B\geq\hat{\eta}>0$.

Expanding the integrand in (50)

$$H_n=\frac{1}{\pi}\int_{2\pi}\sum_{k=1}^{\infty}\frac{(-1)^{k-1}}{k}\times\exp[-k(\hat{\eta}\cos\varphi+B)-in\varphi]d\varphi\ , \tag{60}$$

results in a Taylor series converging by validity of (44). The following derivation is analogous to the correction of G_n,

$$H_n=2(-1)^n\sum_{k=1}^{\infty}\frac{(-1)^{k-1}}{k\exp(kB)}I_0(k\hat{\eta})=\frac{2(-1)^n}{\sqrt{2\pi\hat{\eta}}}\sum_{k=1}^{\infty}\exp[k(\hat{\eta}-B)]\frac{(-1)^{k-1}}{k^{3/2}}\ . \tag{61}$$

At $D=1$ the series was evaluated numerically (and rounded),

$$K_2=\sum_{k=1}^{\infty}\frac{(-1)^{k-1}}{k^{3/2}}=0.7651\ . \tag{62}$$

The approximate formula, giving exact values for $\hat{\eta}=B$ $(D=1)$ and $B/\hat{\eta}\to\infty$ $(D\to0)$ analogous to (46), can be expressed at intermediate values of B by

$$\sum_{k=1}^{\infty}\frac{(-1)^{k-1}}{k^{3/2}}D^k\approx\frac{1}{K_2^*+1/D}\ , \tag{63}$$

where $K_2^*=1/K_2-1=0.3069$, and provides, finally, for finite $\hat{\eta}$ and $B\geq\hat{\eta}$

$$H_n=\frac{2(-1)^n}{\sqrt{2\pi(\hat{\eta}-1/3)}[K_2^*+\exp(B-\hat{\eta})]} \tag{64}$$

and, for $-B\geq\hat{\eta}>0$ using (59),

$$H_n=-2\delta_{0n}B-\delta_{1n}\hat{\eta}+\frac{2}{\sqrt{2\pi(\hat{\eta}-1/3)}[K_2^*+\exp(-B-\hat{\eta})]}\ . \tag{65}$$

These relations show that the error of the asymptotic solution for $|B|<\hat{\eta}$ is, instead of $O(\hat{\eta}^{-1})$ given by (58) for $|B|<\hat{\eta}$, of $O(\hat{\eta}^{-1/2})$. Analogous to the improvement of G_n, formula (64) is a suitable approximation outside the convergence domain $(B\geq\hat{\eta})$ also. Hence, the matching point B^* can be taken from the derivation concerning G_n, so that $B^*=\hat{\eta}-1$.

B. Discharge current

For $|B|<\hat{\eta}$ the discharge current (13) consists of nearly two rectangular waves with a height of 1 and $-\alpha$, and a pulse duty factor depending on B (see Fig. 2). Due to the jumps, the amplitude of the harmonics decreases with $1/n$ in agreement to (34). The periodic averaged discharge current, including the correction at $B\approx\hat{\eta}$,

$$\overline{\Gamma}=\begin{cases}-\alpha+\dfrac{1+\alpha}{\sqrt{2\pi(\hat{\eta}-1/3)}[K_1^*+\exp(-\eta_B-\ln a-\hat{\eta})]}, & \forall B<1-\hat{\eta},\\ 1-\dfrac{1+\alpha}{\pi}\arccos\dfrac{\eta_B+\ln a}{\hat{\eta}}-O(\hat{\eta}^{-2}), & \forall|B|\leq\hat{\eta}-1\\ 1-\dfrac{1+\alpha}{\sqrt{2\pi(\hat{\eta}-1/3)}[K_1^*+\exp(\eta_B+\ln a-\hat{\eta})]}, & \forall B>\hat{\eta}-1\end{cases} \tag{66}$$

follows from (28) and $G_0/2$ according to (33), (47), and (48) $(K_1^*=0.6532)$. The dependence of $\overline{\Gamma}$ on η_B is shown in Fig. 3, for a pure diode configuration $(\alpha=\alpha_1=3)$. The error of the corrected asymptotic solution (66) is, even for small rf amplitudes $(\hat{\eta}\approx20)$, less than 1%.

In the inner interval $|B|\leq\hat{\eta}-1$, Eq. (66) reduces to

$$\overline{\Gamma}=1-(1+\alpha)\left[1-\frac{\tilde{\varphi}}{\pi}\right], \tag{67}$$

where the angle of current flow $\tilde{\varphi}$ is defined by (30) and results in

$$\tilde{\varphi}=\pi\frac{\alpha+\overline{\Gamma}}{\alpha+1}\ . \tag{68}$$

Equation (17) yields in conjunction with (28) and the Fourier series G_n (see Sec. III A) the frequency spectrum of the current drawn by an arbarity electrode. Particularly the dependence of the periodic averaged current $\overline{\Gamma}_m$, Eq. (17), in time average, and of the potential $\eta_H^{(m)}$, Eq. (19), on the bias voltage η_B can be shown. From (28), (34), and (68) the Fourier series of discharge current can

be written in terms of the average discharge current $\bar{\Gamma}$,

$$\Gamma-\bar{\Gamma}=(1+\alpha)\frac{2}{\pi}\sum_{n=1}^{\infty}\frac{1}{n}\sin\left[n\pi\frac{\alpha+\bar{\Gamma}}{\alpha+1}\right]\cos n\varphi\ . \tag{69}$$

C. Bias voltage

The inverse relation of (66) provides the bias voltage η_B as a function of the average current $\bar{\Gamma}$,

$$\eta_B=\begin{cases}-\hat{\eta}-\ln\left[\dfrac{1+\alpha}{(1-\bar{\Gamma})\sqrt{2\pi(\hat{\eta}-1/3)}}\right]-\ln a, & \forall\bar{\Gamma}<\bar{\Gamma}^*_- \\ \hat{\eta}\sin\left[\dfrac{\pi}{2}\dfrac{\alpha-1+2\bar{\Gamma}}{\alpha+1}\right]-\ln a+O(\hat{\eta}^{-1}), & \forall\bar{\Gamma}\in[\bar{\Gamma}^*_-,\bar{\Gamma}^*_+] \\ \hat{\eta}+\ln\left[\dfrac{1+\alpha}{(1-\bar{\Gamma})\sqrt{2\pi(\hat{\eta}-1/3)}}\right]-\ln a, & \forall\bar{\Gamma}<\bar{\Gamma}^*_+\ .\end{cases} \tag{70}$$

At the matching point $B=1-\hat{\eta}$ the average current is

$$\bar{\Gamma}^*_-=-\alpha+\frac{1+\alpha}{\sqrt{2\pi(\hat{\eta}-1/3)}[K_1^*+\exp(-1)]}$$
$$\approx-\alpha+\frac{1+\alpha}{\sqrt{2\pi\hat{\eta}}} \tag{71}$$

and at $B=\hat{\eta}-1$

$$\bar{\Gamma}^*_+=1-\frac{1+\alpha}{\sqrt{2\pi(\hat{\eta}-1/3)}[K_1^*+\exp(-1)]}$$
$$\approx1-\frac{1+\alpha}{\sqrt{2\pi\hat{\eta}}}\ . \tag{72}$$

Reduction to the inner interval provides for the bias voltage η_B

$$\eta_B=-\hat{\eta}\cos\tilde{\varphi}-\ln a\ , \tag{73}$$

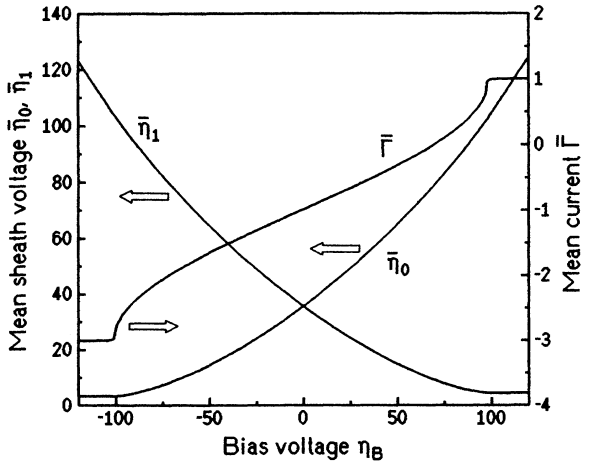

FIG. 3. Mean sheath voltage and mean discharge current vs bias voltage ($\hat{\eta}=100$, $\eta_f=4.7$). The ion current ratio α was supposed to be independent of the bias voltage ($\alpha=3$).

where the angle of current flow $\tilde{\varphi}$ can be calculated by using (68). The term $\ln a$, which was introduced to be a function of the electrode potentials, can be replaced by (18).

For a discharge without dc current $\bar{\Gamma}=0$, e.g., capacitive coupling, Eq. (70) reduces for

$$\frac{1}{\sqrt{2\pi\hat{\eta}}-1}<\alpha<\sqrt{2\pi\hat{\eta}}-1 \tag{74}$$

to the linear relationship

$$\eta_B=\hat{\eta}\sin\left[\frac{\pi}{2}\frac{\alpha-1}{\alpha+1}\right]-\ln a \tag{75}$$

of bias voltage and rf amplitude in agreement to experimental results given in Ref. [13]. Using $\bar{\Gamma}=0$ Eq. (70) yields the complete representation.

Only pure configurations ($a=\alpha=\alpha_i$) without dc current ($\bar{\Gamma}=0$) have been treated by the known models. Köhler, Horne, and Coburn have presented a similar formula based on a simple derivation [13]. Other solutions or approximations are not satisfactory. Suzuki and coworkers gave an approximation based on a Taylor expansions without proof of convergence [16]. For analogous expansions the convergence domain was located outside the interval (74) which does not appear realistically for a pure configuration excluding additional dc currents and electrodes. Pointu presents incomplete approximations only [14]. The approximation given by Vallinga and de Hoog [15], which is an improvement of the relation used by Godyak and Kuzovnikov [10], are not suited for the whole parameter region. Furthermore, it does not excite the influence of the symmetry parameter $a=\alpha$ and the electron temperature [here by $\ln a=\ln\alpha$ in (75)] sufficiently. Using Eq. (38) estimates the small error of (75) to be

$$\Delta\eta_B \approx -\frac{2B}{\hat{\eta}^2-B^2} \approx -\frac{2}{\hat{\eta}}\left[\sin\frac{\pi}{2}\frac{\alpha-1}{\alpha+1}/\cos^2\frac{\pi}{2}\frac{\alpha-1}{\alpha+1}\right] \tag{76}$$

and leads to the relative error $\Delta\eta_B/\eta_B = -O(\hat{\eta}^{-2})$.

D. Sheath voltage

Before discussing the time-averaged sheath voltages, the first harmonics of η_m are presented. For a pure dipole configuration ($l=1$) η_1 will be called plasma potential. Using Eq. (9), the harmonics of η_0 can be derived easily. For $|B| \le \hat{\eta}-1$, or by the validity of (74), and for pure configurations, the first harmonics of η_m ($m \ge 1$) can be expressed as follows:

$$H_1 = \hat{\eta}\left[\frac{\tilde{\varphi}}{\pi} - 1 - \frac{\sin 2\tilde{\varphi}}{2\pi}\right], \tag{77}$$

$$H_2 = \frac{2\hat{\eta}}{3\pi}\sin^3\tilde{\varphi}, \tag{78}$$

$$H_3 = \frac{\hat{\eta}}{6\pi}\sin 2\tilde{\varphi}(1-\cos 2\tilde{\varphi}). \tag{79}$$

The following harmonics can be calculated from (54). Since, for $\hat{\eta}\to\infty$, the sheath voltage is not smooth with respect to φ (see Fig. 2), the Fourier coefficients H_n decrease roughly with n^{-2}. The maximum and the minimum of the sheath voltage determine the upper and the lower bounds of the ion energy distribution. They can be calculated from Eqs. (23) and (24). For example, the maximum of η_0 is located at $\varphi=0$ and can be approximated by $\max\eta_0 \approx \max\eta_q + \ln a = \hat{\eta}+\eta_B+\ln a$, as can be seen from Fig. 2. The qualitative oscillogram of η_0 shown in this figure is in agreement with experimental results given in Ref. [6].

From (49) and H_0 according to (56), (64), and (65), the mean sheath voltage can be written as a function of the bias voltage

$$\bar{\eta}_0 = \begin{cases} \eta_f - \ln(\alpha+1) + \dfrac{1}{\sqrt{2\pi(\hat{\eta}-1/3)}[K_2^* + \exp(-B-\hat{\eta})]}, & \forall B < 1-\hat{\eta} \\ \eta_f - \ln(\alpha+1) + \dfrac{1}{\pi}\left[(\hat{\eta}^2-B^2)^{1/2} + B\arccos\dfrac{B}{\hat{\eta}}\right] + O(\hat{\eta}^{-1}), & \forall |B| \le \hat{\eta}-1 \\ \eta_f - \ln(\alpha+1) + B + \dfrac{1}{\sqrt{2\pi(\hat{\eta}-1/3)}[K_2^* + \exp(B-\hat{\eta})]}, & \forall B > \hat{\eta}-1, \end{cases} \tag{80}$$

where $B=\eta_B+\ln a$ and $K_2^*=0.3069$. From (9) the analogous representation for $\bar{\eta}_m$ can be obtained by time averaging (9).

To verify that the corrected asymptotic solution satisfies the general relation (25), it suffices to prove that $dB/d\eta_B = 0$ using (22).

The dependence of the sheath voltages, both η_0 and η_1, on the bias voltage η_B is shown in Fig. 3 for a pure diode configuration ($\alpha=\alpha_1=3$). The Fourier spectrum normalized by the rf amplitude (peak voltage) from the ion current ratio α is shown in Fig. 4. This representation does not depend on the rf amplitude $\hat{\eta}$.

Substituting the bias voltage η_B by (70), one obtains an appropriate function in $\bar{\Gamma}$. At moderate values of η_B, strictly speaking $|B| \le \hat{\eta}-1$, and large rf voltages $\hat{\eta}^{1/2} \gg 1$, Eq. (80) can be reduced to the asymptotic solution (see Sec. III A) without substantial loss of accuracy,

$$\bar{\eta}_0 = \eta_f - \ln(1+\alpha) + \hat{\eta}\left[\frac{\sin\tilde{\varphi}}{\pi} - \frac{\tilde{\varphi}}{\pi}\cos\tilde{\varphi}\right], \tag{81}$$

$$\bar{\eta}_m = \eta_f - \eta_H^{(m)} + \ln\frac{a}{1+\alpha} + \hat{\eta}\left[\frac{\sin\tilde{\varphi}}{\pi} + \left(1-\frac{\tilde{\varphi}}{\pi}\right)\cos\tilde{\varphi}\right],$$

where $\tilde{\varphi}$ is defined by (30) again. For pure configurations ($a=\alpha=\alpha_1$) without an additional dc current ($\bar{\Gamma}=0$) similar solutions have already been presented [13,15]. These solutions and other approximations [14,16], how-

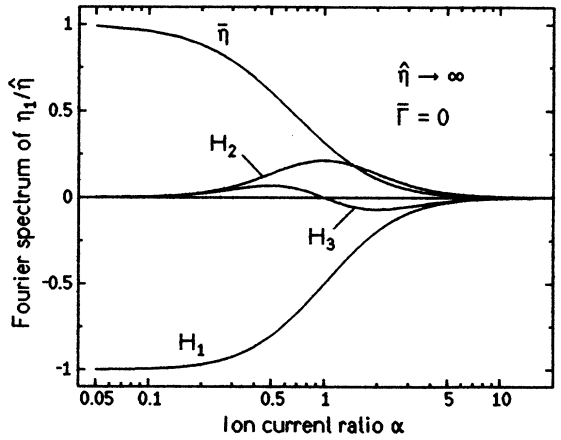

FIG. 4. Fourier coefficients of the first harmonics vs ion current ratio $\alpha=a$. In this case, $\hat{\eta}=\eta_f-\ln\alpha/(\alpha+1)+H_0/2$ [see Eq. (82)].

ever, are not based on an asymptotic solution as given in Sec. III A. Due to the general relation between the Fourier expansions of discharge current and sheath voltage (52), the properties of (80) and (81) are substantially the same as that concerning discharge current and bias voltage.

From (68) the corresponding relation in terms of Γ can be obtained easily. If there is no additional dc current ($\bar{\Gamma}=0$), and the weak condition (74) is satisfied, the final result is

$$\bar{\eta}_0=\eta_f+\ln\frac{1}{1+\alpha}+\hat{\eta}\left[\frac{1}{\pi}\cos\left[\frac{\pi}{2}\frac{\alpha-1}{\alpha+1}\right]+\frac{\alpha}{1+\alpha}\sin\left[\frac{\pi}{2}\frac{\alpha-1}{\alpha+1}\right]\right],$$
$$\bar{\eta}_m=\eta_f-\eta_H^{(m)}+\ln\frac{a}{1+\alpha}+\hat{\eta}\left[\frac{1}{\pi}\cos\left[\frac{\pi}{2}\frac{\alpha-1}{\alpha+1}\right]-\frac{1}{1+\alpha}\sin\left[\frac{\pi}{2}\frac{\alpha-1}{\alpha+1}\right]\right]. \quad (82)$$

The term $\ln a$ involves the electrode potentials. Writing in terms of the average discharge current $\bar{\Gamma}=\bar{\Gamma}_0$ and average current of an arbitrary electrode $\bar{\Gamma}_m$, the term $\ln a$ can be replaced in conjunction with (18). For the electrode with constant current Γ^* the sheath voltage

$$\eta^*=\eta_f-\ln\left[1-\frac{\Gamma^*}{\alpha^*}\right] \quad (83)$$

is constant in time and gives rise to the time-dependent electrode potential

$$\eta_H^*=\eta_m+\eta_H^{(m)}-\eta_f+\ln\left[1-\frac{\Gamma^*}{\alpha^*}\right] \quad (84)$$

reduced to the sheath voltage of an arbitrary electrode $m\neq 0$.

E. Power balance

Knowing the mean sheath voltages, we can directly calculate the total power imparted to the plasma. To investigate this quantitatively, we restrict ourselves to the simple case of a diode system ($l=1$). Usually the rf peak voltage is much higher than the floating potential ($\hat{\eta}/\eta_f \gg 1$). Therefore the thermal (but not the secondary) electron current can be neglected, and the power is given by

$$P=U_T I_{is}^{(0)}(1+\gamma_i)(\eta_0+\alpha\eta_1). \quad (85)$$

γ_i is the (second Townsend) coefficient of secondary-electron emission which here is supposed to be independent of the ion energy. By using the conditions $\hat{\eta}/\eta_f \gg 1$ and (74) the floating potential can be neglected in (81). The expression $\eta_B\bar{\Gamma}$ in the relation for the time-averaged power, obtained from (68) and (81),

$$\bar{P}=\frac{\hat{U}}{\pi}I_{is}^{(0)}(1+\alpha)(1+\gamma_i)\sin\left[\pi\frac{1-\bar{\Gamma}}{\alpha+1}\right]+\eta_B\bar{\Gamma} \quad (86)$$

can be identified as the dc power imparted by the external bias-voltage source.

For the sake of simplicity, we now consider only the pure case of no external dc current ($\bar{\Gamma}=0$). Replacing α [compare (5) and (75)] leads to

$$\bar{P}=\frac{1}{\pi}(I_{is}^{(0)}+I_{is}^{(1)})(1+\gamma_i)(\hat{U}^2-U_B^2)^{1/2}. \quad (87)$$

If we assume the secondary electrons to be the main source of ionization [50], we can neglect power dissipation and ionization by bulk electrons. At the right-hand side of the inequality following from the power balance of secondary electrons

$$\bar{P}_e=\frac{\gamma_i\hat{U}}{\pi}(I_{is}^{(0)}+I_{is}^{(1)})\cos\frac{\pi}{2}\frac{\alpha-1}{\alpha+1}>U_I(I_{is}^{(0)}+I_{is}^{(1)}), \quad (88)$$

we have taken into consideration energy losses due to ionizing collisions using the ionization potential U_I. Thus we only regard inelastic collisions which are directly coupled to particle losses at walls and electrodes. This results in a lower bound of the rf peak voltage

$$\hat{U}>\frac{\pi U_I}{\gamma_i}\left[\cos\frac{\pi}{2}\frac{\alpha-1}{\alpha+1}\right]^{-1}. \quad (89)$$

Obviously, a symmetrical discharge ($\alpha\approx 1$) is most efficient. For example, for an Ar discharge ($U_I=15.8$ V), $\gamma_i\approx 0.1$ [35,51], and $\alpha\approx 1$, we obtain $\hat{U}>500$ V.

Since we have excluded other inelastic collisions of electrons, e.g., excitation, and electrons traversing the plasma without full loss of their kinetic energy, the validity of (89) for a self-maintained discharge is only necessary, but not sufficient. Note that (89) can be violated, if ionization by thermal electrons cannot be neglected [50], e.g., for high electrode spacing $2L$ or high pressure.

IV. EXTENSION OF THE RESISTIVE MODEL

The above model is not intended to imply that, depending on discharge conditions, the assumption of the same electron temperature at every sheath boundary can be violated. Experimental results from unsymmetrical discharges ($|\eta_B/\hat{\eta}|\sim 1$) exhibit a higher electron temperature according to a larger sheath voltage at the smaller electrode [6,28,49,52,53]. Since this problem can hardly be involved in the general solution, it is treated separately.

Already being included in the ion current ratio α_k [see Eq. (5)], different densities do not require an extension of the resistive model given in the last section.

We assume equal electron temperature on the lower side in $U_{Tk}=U_{Tl}$ and, usually, a higher one on the upper

side $U_{T0} \neq U_{Tl}$ in Fig. 1. Defining the temperature parameter Θ

$$\Theta = \frac{U_{T0} - U_{T1}}{U_{T0}} = 1 - \frac{U_{T1}}{U_{T0}} \tag{90}$$

and normalizing the sheath voltages with respect to U_{T0}, instead of U_T in (4), yields in extension of (10)

$$0 = \Gamma^* + \exp(\eta_f - \eta_0) + \sum_{k=0}^{l} \alpha_k - \sum_{k=1}^{l} \alpha_k \exp\left[\eta_f - \frac{\eta_k}{1-\Theta}\right] . \tag{91}$$

The definition of the integral symmetry parameter a can now be extended

$$a = \sum_{k=1}^{l} \alpha_k \exp\left[\frac{\eta_H^{(k)}}{1-\Theta}\right] , \tag{92}$$

where $\eta_H^{(k)}/(1-\Theta) = u_H^{(k)}/U_{T1}$. The current of an arbarity electrode, in extension of (17),

$$\frac{\Gamma_m}{\alpha_m} = 1 - \frac{\alpha + \Gamma}{a} \exp\left[\frac{\eta_H^{(m)}}{1-\Theta}\right] . \tag{93}$$

The equation can now be used to express $\ln a$ as

$$\ln a = \frac{\eta_H^{(m)}}{1-\Theta} + \ln \frac{\alpha + \bar{\Gamma}}{1 - \bar{\Gamma}_m/\alpha_m} . \tag{94}$$

Instead of Eq. (11), one obtains an indirect representation of the sheath voltage η_0,

$$0 = 1 + \alpha - \exp(\eta_f - \eta_0)\left[1 + a \exp\left[\frac{\eta_q - \Theta\eta_0}{1-\Theta}\right]\right] , \tag{95}$$

which cannot be resolved analytically. Therefore, as follows from (6), the analogous equation for $\Gamma = \Gamma_0$ can only be resolved numerically also. Extending the definition of B according to (14)

$$B = \eta_B + \ln a - \Theta\left[\eta_f + \ln \frac{a}{1+\alpha}\right] \tag{96}$$

and rearranging (95)

$$\eta_0 = \eta_f - \ln(1+\alpha) + \ln\left[1 + \exp\left[\frac{\eta_q - \Theta\eta_0}{1-\Theta} + \ln a\right]\right] , \tag{97}$$

the sheath voltage can be represented, for sufficiently large rf voltage, strictly speaking $\hat{\eta} \to \infty$ and $\Theta \neq 1$, by the steady asymptotic function

$$\eta_0 = \begin{cases} \eta_f - \ln(1+\alpha) + \eta_{\mathrm{rf}} + B, & \forall \varphi \in \left[0, \frac{\bar{\varphi}}{2}\right] \\ \eta_f - \ln(1+\alpha), & \forall \varphi \in \left[\frac{\bar{\varphi}}{2}, \pi\right] , \end{cases} \tag{98}$$

which can be written as

$$\eta_0 = \eta_f - \ln(1+\alpha) + \eta_{\mathrm{rf}} + B + \ln\{1 + \exp(-\eta_{\mathrm{rf}} - B)\} . \tag{99}$$

In conjunction with (6) this asymptotic representation yields Eqs. (13) and (23) again. Thus the Fourier coefficients for the discharge current in (28) and for the sheath voltage in (49) can be calculated by using B according to (96). For bias voltages, which do not exceed the rf peak voltage, strictly speaking $|B| \leq \hat{\eta} - 1$, the mean sheath voltage can be expressed as

$$\bar{\eta}_0 = \eta_f - \ln(1+\alpha) + \hat{\eta}\left[\frac{\sin\bar{\varphi}}{\pi} - \frac{\bar{\varphi}}{\pi}\cos\bar{\varphi}\right] , \tag{100}$$

$$\bar{\eta}_m = (1-\Theta)\left[\eta_f - \eta_H^{(m)} + \ln \frac{a}{1+\alpha}\right] + \hat{\eta}\left[\frac{\sin\bar{\varphi}}{\pi} + \left[1 - \frac{\bar{\varphi}}{\pi}\right]\cos\bar{\varphi}\right] .$$

As the last equation shows, only the dc part of sheath voltage, concerning particularly the floating potential, declines with lower electron temperature ($\Theta > 0$). In the case in which $\hat{\eta} \gg \eta_f$, e.g., suggested by (89), the rf part is not influenced compared to $\Theta = 0$.

A discharge without an additional dc current ($\bar{\Gamma} = 0$) provides in conjunction with condition (74)

$$\eta_B = \hat{\eta} \sin\left[\frac{\pi}{2}\frac{\alpha - 1}{\alpha + 1}\right] - \ln a + \Theta\left[\eta_f + \ln \frac{a}{1+\alpha}\right] \tag{101}$$

a linear relation between rf peak voltage $\hat{\eta}$ and bias voltage η_B again. For $\Theta \to 0$ we recover (75), as expected.

Different electron temperatures ($\Theta \neq 0$) cause only different floating potentials essentially. It is not difficult to show that also the assumption of the Boltzmann relation and a possible modulation of electron temperature are not substantial from this point of view. The nonnormalized floating potential $\varphi_f = U_T \eta_f$ can be approximated by the time-averaged electron temperature.

V. RESULTS AND DISCUSSION

The asymptotic solution is shown to be a suitable approach and of high accuracy. At large rf amplitudes $\hat{\eta}$ (peak voltage) and without dc current, the linear dependences of bias voltage and sheath voltage on the rf amplitude, already known for pure configurations without dc current and additional electrodes, are found. For bias voltages below a critical value the error was estimated to be of $O(\hat{\eta}^{-2})$ for the discharge current, and of $O(\hat{\eta}^{-1})$ for both bias and sheath voltage. The relation of the average discharge current and an external bias voltage shows the strong nonlinearity of the rf discharge and the possibility of controlling of the average sheath voltage (see Fig. 3). For a capacitivly coupled discharge, the nonlinearity can be well demonstrated by the Fourier spectrum in Fig. 4.

In the case of one auxiliary electrode, and if the driven electrode is coupled capacitivly, the average current is essentially the same as found in theory and experiment in the range well above ω_{pi} [3,28]. In this case Eq. (17) reduces in time average to

$$\frac{\bar{\Gamma}_2}{\alpha_2}=1-\frac{\alpha_1+\alpha_2}{\alpha_1\exp(-\eta_H)+\alpha_2} \tag{102}$$

and indicates that the auxiliary [2] and grounded [1] electrode can be interpreted as a double-probe system, even for arbitrary rf voltages.

The bias voltage η_B was shown to be a linear measure of the change of the average plasma potential (sheath voltage of the first electrode) caused by a slowly varying potential of the auxiliary electrode.

ACKNOWLEDGMENTS

I wish to thank Dr. W. Rehak for his encouragement and valuable comments throughout the course of this work. I am also grateful to K. Börnig, F. Heinrich, P. Hoffmann, and H. Mischke for stimulating discussions.

APPENDIX

In particular, the modulation of ion current has to be considered in (13) for the discharge current. Because of the time-independent plasma density, see physical assumptions, the sum of the ion currents is only weakly modulated and can assumed to be constant [29]. Rewriting the non-normalized Eqs. (13) and (7),

$$\bar{I}=I_{is}^{(0)}-\frac{\sum_{k=1}^{l} I_{is}^{(k)}+I^*}{1+\exp(\eta_q+\ln a)}\ , \tag{A1}$$

this sum appears as constant factor. The non-normalized constant current I^* refers to Γ^* in Fig. 1. After time averaging (dc current, bias voltage) only the average ion current has to be taken into account. The remaining weak logarithmic dependence in η_f and $\ln a$, e.g., for the sheath voltage, can be neglected. Thus all expressions remain valid, at least approximately.

[1] T. Okuda and K. Yamamoto, J. Appl. Phys. **31**, 158 (1960).
[2] J. W. Coburn and E. Kay, J. Appl. Phys. **43**, 4965 (1972).
[3] P. Hoffmann, M. Kammeyer, and M. Klick, in *Proceedings of the Tenth International Symposium on Plasma Chemistry,* edited by U. Ehlemann, H. G. Lergon, and K. Wiesemann (IUPAC, Bochum, Germany, 1991), Vol. 2, abstract 2.1-11.
[4] A. P. Paranjpe, J. P. McVittie, and S. A. Self, J. Appl. Phys. **67**, 6718 (1990).
[5] D. Maundrill, J. Slatter, A. I. Spiers, and C. C. Welch, J. Phys. D **20**, 815 (1987).
[6] C. A. Anderson, W. G. Graham, and M. B. Hopkins, Appl. Phys. Lett. **52**, 783 (1988).
[7] C. M. Horwitz and T. Puzzer, J. Vac. Sci. Technol. A **8**, 3123 (1990).
[8] K. Matsumoto and M. Sato, J. Appl. Phys. **54**, 1781 (1983).
[9] O. Auciello and D. L. Flamm, *Plasma Diagnostics* (Academic, London, 1989), Vol. 1, pp. 164–168.
[10] V. A. Godyak and A. A. Kuzovnikov, Fiz. Plazmy **1**, 3 (1975) [Sov. J. Plasma Phys. **1**, 278 (1975)].
[11] R. H. Bruce, J. Appl. Phys. **52**, 7064 (1981).
[12] C. M. Horwitz, J. Vac. Sci. Technol. A **1**, 60 (1983).
[13] K. Koehler, D. E. Horne, and J. W. Coburn, J. Appl. Phys. **58**, 3350 (1985).
[14] A. M. Pointu, J. Appl. Phys. **60**, 4113 (1986).
[15] P. M. Vallinga and F. J. de Hoog, J. Phys. D **22**, 925 (1989).
[16] K. Suzuki *et al.*, Jpn. J. Appl. Phys. **25**, 1569 (1986).
[17] V. A. Godyak and N. Sternberg, IEEE Trans. Plasma Sci. **18**, 159 (1990).
[18] H. S. Buttler and G. S. Kino, Phys. Fluids **6**, 1346 (1963).
[19] W. D. Davis and T. A. Vanderslice, Phys. Rev. **131**, 219 (1963).
[20] A. Metze, D. W. Ernie, and H. J. Oskam, J. Appl. Phys. **60**, 3081 (1986).
[21] D. Bohm, in *Characteristics of Electrical Discharges in Magnetic Fields,* edited by A. Guthrie and R. Wakering (McGraw-Hill, New York, 1949), p. 77.
[22] K.-U. Riemann, Ph.D. thesis, University Bochum, Germany, 1977, Report No. 87-02-021 SFB 162 Bochum/Jülich (unpublished).
[23] K.-U. Riemann, Phys. Fluids **24**, 2163 (1981).
[24] K.-U. Riemann, J. Phys. D **24**, 493 (1991).
[25] R. Deutsch and E. Räuchle, in *Proceedings of the Tenth European Sectional Conference on the Atomic and Molecular Physics of Ionized Gases,* edited by B. Dubreuil (European Physical Society, Orleans, France, 1990), abstract 6-15.
[26] P. R. Smy and J. R. Greig, J. Phys. D **1**, 351 (1968).
[27] P. R. Smy, J. A. Nation, and D. Simpson, J. Phys. D **2**, 1095 (1969).
[28] M. Klick, Ph.D. thesis, University Greifswald, Germany, 1991 (unpublished).
[29] W. J. Goedheer and P. M. Meijer, IEEE Trans. Plasma Sci. **19**, 245 (1991).
[30] R. A. Gottscho, Phys. Rev. A **36**, 2233 (1987).
[31] The application of the results derived in this paper can be extended to electronegative plasmas if, because of low temperature far below the potential within the sheath, the negative ions are not be able to leave the bulk plasma (e.g., for sufficiently low pressure). R. L. F. Boyd and J. B. Thompson, Proc. R. Soc. London **252**, 102 (1959).
[32] W. P. Allis and D. J. Rose, Phys. Rev. **93**, 84 (1954).
[33] V. E. Golant, A. P. Zhilinsky, and I. E. Sakharov, *Fundamentals of Plasma Physics* (Wiley, New York, 1980), pp. 63–66, 150–152, and 209–226.
[34] R. A. Gottscho *et al.*, J. Appl. Phys. **55**, 2707 (1984).
[35] S. C. Brown, *Basic Data of Plasma Physics,* 1966 (MIT Press, London, 1967), pp. 47–79 and 218–235.
[36] E. W. McDaniel, *Collision Phenomena in Ionized Gases* (Wiley, New York, 1964), pp. 251–260.
[37] V. A. Godyak, *Soviet Radio Frequency Discharge Research*

(Delphic Associates, Falls Church, 1986), p. 86.
[38] L. S. Frost, Phys. Rev. **105**, 354 (1957).
[39] The underlying calculations do not imply ionization by secondary electrons. Since $1/\nu_D$ can be used to estimate the time constant of plasma decay, independent of source of ionization, condition (1) should be valid also in this case (Refs. [28,33]).
[40] R. Winkler, H. Deutsch, J. Wilhelm, and Ch. Wilke, Beitr. Plasmaphys. **24**, 285 (1984).
[41] V. M. Donnely and D. L. Flamm, J. Appl. Phys. **58**, 2135 (1985).
[42] T. Makabe and M. Nakaya, J. Phys. D **20**, 1243 (1987).
[43] R. J. Seeböck and W. E. Köhler, J. Appl. Phys. **64**, 3855 (1988).
[44] S. A. Self, Phys. Fluids **6**, 1762 (1963).
[45] J. H. Ingold, Phys. Fluids **15**, 75 (1972).
[46] G. K. Bienkowski, Phys. Fluids **10**, 381 (1967).
[47] K.-B. Pearsson, Phys. Fluids **5**, 1625 (1962).
[48] S. A. Self and H. N. Ewald, Phys. Fluids **9**, 2486 (1966).
[49] H. Sabadil, S. Klagge, and M. Kammeyer, Plasma Chem. Plasma Proc. **8**, 425 (1988).
[50] V. A. Godyak and A. S. Khanneh, IEEE Trans. Plasma Sci. **14**, 112 (1986).
[51] P. F. Little, in *Handbuch der Physik,* edited by H. Flügge (Springer, Berlin, 1956), Vol. XXI, pp. 638–647.
[52] T. Kaneda *et al.*, J. Phys. D **23**, 1642 (1990).
[53] G. Dilecce, M. Capitelli, and S. De Benedictis, J. Appl. Phys. **69**, 121 (1991).